MECH876-Intelligent Vehicle Control Systems
Project Report

Unscented Kalman Filter based Super Twisting Control for a Half-car Suspension System

Duc-Giap Nguyen - 2022324052

Kyoungtae Ji - 2022222145

May 30, 2022

1 Abstract

A good suspension system is of paramount importance to the operating performance of a vehicle and, consequently, to the safety and driving comfort of passengers. Nevertheless, suspension systems are susceptible to nonlinearity, parameter uncertainty, and exogenous perturbation, which can easily impair their effectiveness. Thus, nonlinear controllers with high robustness such as sliding mode control (SMC) are normally selected to control the suspensions. This study first employs a full state feedback super twisting control (FS-STC) to stabilize both vertical displacement and pitch angle of a half-car suspension system. FS-STC inherits the robust property of SMC while effectively attenuating chattering phenomenon as one of its attractive features. However, FS-STC strictly requires displacement and velocity state feedback, which implies additional sensors have to be installed, thus increasing the complexity in the physical structure and being prone to noisy measurement. Therefore, a higher order sliding mode observer (HOSMO) based STC (HOSMO-STC) and an unscented Kalman filter (UKF) based STC (UKF-STC) are subsequently proposed to tackle this problem. HOSMO estimates velocity states thus reducing the dependence on state feedback for STC design. Meanwhile, UKF takes further actions by utilizing more common and easily accessible relative displacement such as suspension stroke to estimate all system states, reconstruct internal dynamics and disturbance, and subsequently use them for the control design process. As a result, the comparative simulation in this study demonstrates that UKF-STC offers better performance in terms of both convergence accuracy and chattering alleviation compared to FS-STC and HOSMO-STC. The results suggests that the integration of a nonlinear state estimation algorithm like UKF and a highly robust control algorithm like STC is an effective combination which can be applied to numerous control systems.

2 Introduction

Suspension systems are one of the most important parts of a vehicle, which directly affect vehicle performance in road holding and driving comfort. Placing between the vehicle body and its wheels, a suspension system is responsible for keeping vehicle balanced in various driving scenarios like cornering, accelerating, braking, or driving over a bump/pothole. Therefore, a good suspension system is believed to have a significant impact on the passenger safety, vehicle durability, and maintenance cost. Thus, active suspension systems have received considerable attention from researchers throughout the years [1–4]. While some researchers study on new structures of a suspension system [5], the major concern is on how to design and improve control algorithms for existing physical structures [6, 7].

A primary objective of an active suspension system is to stabilize the attitude of a vehicle in the presence of nonlinearities, parameter uncertainties and external disturbances. Other common objectives include guaranteeing system state constraints so that the criteria of driving comfort and safety can be satisfied. Various control algorithms have been proposed to achieve these goals, for instance, H_∞ [3], backstepping [1, 4], or sliding mode control (SMC) [6, 8], to name just a few.

Backstepping is one of the most popular control approach for suspension systems. An adaptive backstepping control is introduced in [1] to stabilize both vertical and pitch motions of a half-car suspension model. The proposed algorithm accounts for the hydraulic actuator dynamics and also considers parameter variations in the number of passengers. Another backstepping approach can be found in [4], where an integration of adaptive backstepping technique and quadratic Lyapunov function is proposed to stabilize the vehicle while actively addressing the safety constraint of road holding. Both above mentioned papers have an adaptive scheme for parameter adjustment. However, these backstepping algorithm requires full-state measurement of the suspension system, which is costly, prone to measurement noise and even unrealistic regarding complexity in installation space and physical structure of the system. Aware of the full-state sensing problem, a higher order sliding mode control proposed in [6] tried to achieve the stabilization objective by using only the relative suspension displacement such as suspension stroke. This method is believed to be more practical than the full-state based approach since suspension strokes can be obtained easily. However, [6] raises a concern about the stabilization effectiveness as the vertical displacement is controlled indirectly via stabilizing the relative displacement. In fact, it might lack a mathematical justification for its method since zero relative displacement does not have a unique solution. IN other words, even if the relative displacement is driven to zero, the displacements of the vehicle body and the unsprung mass can continue to vary at the same value and only die out gradually because of the stabilizing effects of passive springs and shock absorbers. Therefore, although the utilization of relative suspension displacement is more practical than the use of full-state measurement, the information of the major states such as vertical displacement or pitch angle is still indispensable.

The approach [6] estimate relative velocity and acceleration by a means of a high gain observer. Despite being simplicity, the high gain observer exhibits a drawback of peaking phenomena during transition period [9]. It is also a common belief that high gains might magnify the undesired noise existing in the measured states, thus degrading the overall control performance. On the other hand, the parameter adaptation schemes found in [1, 4] are mathematical sounding but of model-based, implying that the precision of parameter estimation heavily rely on the accuracy of the model. In other words, the discrepancy between the mathematical modeling and the physical system might deteriorate their precision in parameter estimation and overall stabilization performance in practice. These two cases indicate that a control algorithm designated for nonlinear systems, specifically suspension systems, needs to be robust against uncertainty and measurement noise.

From the above motivation, in this study, we compare three control approaches for the objective of stabilization a half-car suspension system while considering about state availability. Three control algorithms including FS-STC, HOSMO-STC and UKF-STC are selected based on their level of dependence on state-feedback information. FS-STC requires both information of direct measurements of displacement and velocity. HOSMO-STC requires only displacement and estimates velocities via HOSMO. Meanwhile, UKF-STC represents an indirect output feedback controller as it utilizes only the relative suspension displacement to estimate all system state, reconstructs inner dynamics and disturbance then uses them for controller design. Their control performance including state stabilization precision, chattering attenuation, road holding and driving comfort are simultaneously evaluated in a comparative simulation.

The rest of the study is organized as follows. Section 3 presents the half-car suspension modeling and control problem statement. Section 4 introduces three proposed control algorithms including FS-STC, HOSMO-STC and UKF-STC. Section 5 provides simulation results and discussion about each controller's advantages and limitations, followed by the conclusion, future work and lessons in Section 6.

3 System Modeling and Problem Statement

3.1 System Description

The half-car suspension system considered in this project is illustrated in Figure 1. In this figure, several parameters used to model the suspension are as follows. M denotes the sprung mass of the vehicle body, and I is the mass moment of inertia associated with the pitch motion. m_f and m_r stand for the

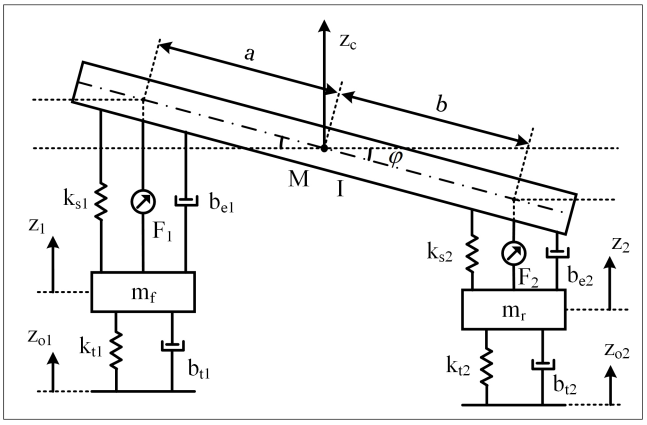

Figure 1: Schematic diagram of the considered half-car suspension system [1].

front and rear unsprung masses, respectively. The stiffness and damping coefficients of the suspension are k_{si} and b_{ei}, $(i = 1, 2)$, respectively. Similarly, k_{ti} and b_{ti}, $(i = 1, 2)$ represent the compressibleness and damping coefficients of the tires, respectively. Motions of the vehicle body are indicated by z_c for the vertical displacement and φ for its pitch angle. While z_1 and z_2 are the displacements of the unsprung mass, z_{o1} and z_{o2} are the road inputs to the wheels of the given model, accordingly. Active control actions enter the system via two forces F_1 and F_2 locating respectively at an distance a and b from the center of mass of the vehicle.

The suspension system is modeled using first principles as follows.

1. Unsprung mass subsystems: these subsystems are modeled as spring-mass-damper systems, whose dynamic equations are given as

$$\begin{cases} m_f\ddot{z}_1 - k_{s1}\Delta y_1 - b_{e1}\Delta\dot{y}_1 + k_{t1}(z_1 - z_{o1}) + b_{t1}(\dot{z}_1 - \dot{z}_{o1}) = -F_1 \\ m_r\ddot{z}_2 - k_{s2}\Delta y_2 - b_{e2}\Delta\dot{y}_2 + k_{t2}(z_2 - z_{o2}) + b_{t2}(\dot{z}_2 - \dot{z}_{o2}) = -F_2 \end{cases} \tag{1}$$

where Δ_{yi} and $\Delta_{\dot{y}i}$, $i = 1, 2$ denote the relative suspension displacements and velocities of the following forms.

$$\Delta y_1 = z_c + a\sin\varphi - z_1, \quad \Delta\dot{y}_1 = \dot{z}_c + a\dot{\varphi}\cos\varphi - \dot{z}_1$$

$$\Delta y_2 = z_c - b\sin\varphi - z_2, \quad \Delta\dot{y}_2 = \dot{z}_c - b\dot{\varphi}\cos\varphi - \dot{z}_2$$

2. Sprung mass subsystems: these subsystems include springs, shock absorbers and actuators that absorb and generate forces between the vehicle body and the road. The dynamics of the sprung mass subsystem can be expressed as

$$\begin{cases} M\ddot{z}_c = -\phi_1(t) + F_1 + F_2 \\ I\ddot{\varphi} = -\phi_2(t) + aF_1 - bF_2 \end{cases} \tag{2}$$

with

$$\phi_1(t) = k_{s1}\Delta y_1 + k_{s2}\Delta y_2 + b_{e1}\Delta\dot{y}_1 + b_{e2}\Delta\dot{y}_2$$
$$\phi_2(t) = a(k_{s1}\Delta y_1 + b_{e1}\Delta\dot{y}_1) - b(k_{s2}\Delta y_2 + b_{e2}\Delta\dot{y}_2)$$

3.2 Problem Statement

The primary objective of the suspension control system is to stabilize the vehicle. Specifically, the control design aims to drive both the vertical displacement, z_c, and the pitch angle, φ, to equilibrium and keep them thereafter.

$$\lim_{t\to\infty} z_c = 0 \quad \text{or} \quad \text{bounded}.$$
$$\lim_{t\to\infty} \varphi = 0 \quad \text{or} \quad \text{bounded}.$$

Other objectives include driving comfort, where vertical and pitch accelerations are kept to relatively small values, and road holding, where the dynamic loads exerted on the tires are regulated not to exceed their static loads. These objectives can be expressed as follows.

$$\left|\frac{k_{ti}(z_i - z_{oi}) + b_{ti}(\dot{z}_i - \dot{z}_{oi})}{S_i}\right| < 1, \quad i = 1, 2 \tag{3}$$

where S_i, $i = 1, 2$ are static loads with following formula:

$$S_1 = \frac{Mgb}{(a+b)} + m_f g \tag{4}$$

$$S_1 + S_2 = (M + m_f + m_r)g. \tag{5}$$

4 Control Algorithm Design

4.1 Control-oriented modeling

The suspension system dynamics expressed at 1 and 2 can be rearranged into a general second-order canonical form as

$$\begin{cases} \dot{X}_1 = X_2 \\ \dot{X}_2 = H\left(X_1, X_2\right) + GU + D \end{cases} \tag{6}$$

where $X_1 = [z_c,\, \varphi]^{\mathrm{T}}$ and $X_2 = [\dot{z}_c,\, \dot{\varphi}]^{\mathrm{T}}$ are the controlled system states, $H\left(X_1, X_2\right)$ denotes the internal dynamics matrix, G is the control matrix, and D represents the lumped disturbance of the following form:

$$\begin{aligned} H &= A_X X_1 + B_X X_2 \\ A_X &= \begin{bmatrix} -(k_{s1} + k_{s2})/M & -(ak_{s1} - bk_{s2})/M \\ -(ak_{s1} - bk_{s2})/I & -\left(a^2 k_{s1} + b^2 k_{s2}\right)/I \end{bmatrix} \\ B_X &= \begin{bmatrix} -(b_{e1} + b_{e2})/M & -(ab_{e1} - bb_{e2})/M \\ -(ab_{e1} - bb_{e2})/I & -\left(a^2 b_{e1} + b^2 b_{e2}\right)/I \end{bmatrix} \\ G &= \begin{bmatrix} 1/M & 1/M \\ a/I & -b/I \end{bmatrix} \\ D &= \begin{bmatrix} k_{s1}/M & k_{s2}/M \\ ak_{s1}/I & -bk_{s2}/I \end{bmatrix} \begin{bmatrix} z_1 \\ z_2 \end{bmatrix} + \begin{bmatrix} b_{e1}/M & b_{e2}/M \\ ab_{e1}/I & -bb_{e2}/I \end{bmatrix} \begin{bmatrix} \dot{z}_1 \\ \dot{z}_2 \end{bmatrix} \\ &\quad + \begin{bmatrix} ak_{s1} - bk_{s2} & ab_{e1} - bb_{e2} \\ a^2 k_{s1} + b^2 k_{s2} & a^2 b_{e1} + b^2 b_{e2} \end{bmatrix} \begin{bmatrix} \sin\varphi - \varphi \\ \dot{\varphi}\left(\cos\varphi - \varphi\right) \end{bmatrix} \end{aligned}$$

It can be interpreted from above matrices that the lumped disturbance D contains unmodeled terms z_i, $\dot{z}_i$, $i = 1, 2$, which we cannot account into the internal dynamics because of the lack of measurement.

4.2 Control candidates

Concerning the availability of displacement/velocity sensing in practice, in this study, the following three controllers are considered.

- Full state feedback super twisting control (FS-STC): both displacement, $[z_c,\, \varphi]^{\mathrm{T}}$, and velocity, $[\dot{z}_c,\, \dot{\varphi}]^{\mathrm{T}}$, measurements are available.
- (Semi-state feedback) Higher order sliding mode observer-based super-twisting control (HOSMO-STC): only displacement, $[z_c,\, \varphi]^{\mathrm{T}}$, is available, and velocity, $[\dot{z}_c,\, \dot{\varphi}]^{\mathrm{T}}$, is estimated using HOSMO.

- (Output feedback) Unscented Kalman filter-based super-twist control (UKF-STC): both displacement, $[z_c, \varphi]^{\mathrm{T}}$, and velocity, $[\dot{z}_c, \dot{\varphi}]^{\mathrm{T}}$, are not available but estimated from relative displacements (suspension strokes), $\Delta_{y1} = z_c + a\sin\varphi - z_1$ and $\Delta_{y2} = z_c - b\sin\varphi - z_2$, using UKF.

4.2.1 FS-STC Formulation

The following linear sliding surface with full information on the displacement and velocity states is considered for the FS-STC.

$$S = C_1 X_1 + X_2 \tag{7}$$

Taking the derivative of the sliding surface 7 and substituting the system dynamics 6 into the derived equation, we obtain:

$$\begin{aligned} \dot{S} &= C_1 \dot{X}_1 + \dot{X}_2 \\ &= C_1 X_2 + (H + GU + D). \end{aligned} \tag{8}$$

Consequently, the following X_1 and S coordinate can be established.

$$\begin{aligned} \dot{X}_1 &= S - C_1 X_1 \\ \dot{S} &= C_1 X_2 + (H + GU + D). \end{aligned} \tag{9}$$

Accordingly, to realize the second-order sliding mode or super-twisting control, a control law can be designed as

$$U = G^{-1}\left(-C_1 X_2 - H - \lambda_1 |S|^{1/2} sign\,(S) - \int_0^t \lambda_2 sign\,(S)\, d\tau\right) \tag{10}$$

where λ_1 and λ_2 are tuning control gains. Substituting the control law 10 into 9, the closed-loop dynamics in X and S coordinate now becomes:

$$\begin{aligned} \dot{X}_1 &= S - C_1 X_1 \\ \dot{S} &= -\lambda_1 |S|^{\frac{1}{2}} sign\,(S) + Z \\ \dot{Z} &= \lambda_2 sign\,(S) + \dot{D}. \end{aligned} \tag{11}$$

If the control gains are properly selected such that $\lambda_1 = 1.5\sqrt{\Delta_1}$ and $\lambda_2 = 1.1\Delta_1$ with $max\left|\dot{D}\right| < \Delta_1$, then the last two equations of 11 forms a super twisting algorithm (STA) [10, 11]. Consequently, the sliding mode, $S = \dot{S} = 0$ will occur, implying that

$$\begin{aligned} \dot{X}_1 &= -C_1 X_1 \\ X_2 &= -C_1 X_1. \end{aligned}$$

Thus, the system states X_1 and X_2 will asymptotically converge to zero.

4.2.2 HOSMO-STC Formulation

The FS-STC design is straight-forward but requires feedback information of vertical and pitch velocities, which can be obtained by velocity sensors or numerical differentiation. However, additional sensors are costly and add complexity to the physical system, and numerical differentiation is prone to measurement noise. Thus, it is more beneficial to implement an observer to estimate the velocities.

An HOSMO formulation [12] is constructed based on the system dynamics 6 as follows:

$$\begin{cases} \dot{\hat{X}}_1 = \hat{X}_2 + Z_1 \\ \dot{\hat{X}}_2 = \hat{X}_3 + \hat{H} + GU + Z_2 \\ \dot{\hat{X}}_3 = Z_3 \end{cases} \tag{12}$$

where $\hat{X}_{1,2}$ are the estimate of system states $X_{1,2}$, and $\hat{X}_3$ estimates the lumped disturbance; $Z_i(i = 1, 2, 3)$ are the correction terms of the forms:

$$Z_1 = \begin{bmatrix} Z_1(1) \\ Z_1(2) \end{bmatrix} = \begin{bmatrix} k_{11}|E_1(1)|^{2/3}\text{sign}(E_1(1)) \\ k_{12}|E_1(2)|^{2/3}\text{sign}(E_1(2)) \end{bmatrix} = K_1|E_1|^{2/3}\text{sign}(E_1) \tag{13}$$

$$Z_2 = K_2|E_1|^{1/3}\text{sign}(E_1) \tag{14}$$

$$Z_3 = K_3\text{sign}(E_1) \tag{15}$$

with $E_1 = X_1 - \hat{X}_1$ being the first estimation error. Other estimation errors include $E_2 = X_2 - \hat{X}_2$, and $E_3 = (H - \hat{H}) + D - \hat{X}_3$. For simplicity, observer gains $K_i(i = 1, 2, 3)$ are selected to be scalars. Consequently, with velocity state estimated from HOSMO, an sliding surface is designed as

$$\hat{S} = C_1X_1 + \hat{X}_2 \tag{16}$$

Differentiating the sliding surface 16 and subsequently applying the system dynamics 6 and the observer dynamics 12, we obtain:

$$\begin{aligned} \dot{\hat{S}} &= C_1\dot{X}_1 + \dot{\hat{X}}_2 \\ &= C_1X_2 + (\hat{X}_3 + \hat{H} + GU + Z_2). \end{aligned} \tag{17}$$

Accordingly, a control law can be designed in the following form.

$$U = G^{-1}\left(-C_1\hat{X}_2 - \hat{X}_3 - \hat{H} + Z_2 - \lambda_1\left|\hat{S}\right|^{1/2}sign(\hat{S}) + \int_0^t \lambda_2 sign(\hat{S})d\tau\right) \tag{18}$$

Taking into account 18, the presence of $\hat{X}_3$ in the control law indicates that HOSMO-STC actively conpensates for the lumped disturbance. Subsequently, applying the above control law into the system, we obtain the following closed-loop dynamics:

$$\begin{aligned} \Xi: &\begin{cases} \dot{E}_1 = -K_1|E_1|^{2/3}sign(E_1) + E_2 \\ \dot{E}_2 = -K_2|E_1|^{1/3}sign(E_1) + E_3 \\ \dot{E}_3 = -K_3sign(E_1) + \dot{D} + (\dot{H} - \dot{\hat{H}}) \end{cases} \\ \Pi: &\begin{cases} \dot{X}_1 = \hat{S} - C_1X_1 + E_2 \\ \dot{\hat{S}} = C_1E_2 - \lambda_1\left|\hat{S}\right|^{1/2}sign(\hat{S}) + Z \\ \dot{Z} = -\lambda_2 sign(\hat{S}) \end{cases} \end{aligned} \tag{19}$$

where Ξ and Π represent the observer error dynamics and X_1-$\hat{S}$ coordinate dynamics, respectively. Investigating Π, it is proved in [12] that the STA will not occur unless the estimation error E_2 is driven to zero first. Therefore, observer gains $K_i(i = 1, 2, 3)$ must be appropriately selected for the finite-time convergence of the observer. For instance, they can be selected as $K_1 = \rho_1L^{1/3}$, $K_2 = \rho_2L^{1/2}$, and $K_3 = \rho_3L$, where $\rho_i\,(i = 1, 2, 3)$ are properly chosen for the observer convergence, and L is the Lipschitz constant of the lumped disturbance/state, which is can be tuned for satisfactory control performance [13]. Once the finite-time convergence of the HOSMO happens, $E_2 = 0$. Substituting this into Π yields:

$$\Pi: \begin{cases} \dot{X}_1 = \hat{S} - C_1X_1 \\ \dot{\hat{S}} = -\lambda_1\left|\hat{S}\right|^{1/2}sign(\hat{S}) + Z \\ \dot{Z} = -\lambda_2 sign(\hat{S}) \end{cases} \tag{20}$$

Provided that $\lambda_i > 0$, $i = 1, 2$ are selected properly, the last two equations of 20 form an STA, and $\hat{S} = \dot{\hat{S}} = 0$ is guaranteed to occur in finite time. Consequently, system states will asymptotically converge

to zeros, as shown in the previous subsection. It is worth noting that unlike FS-STC, HOSMO-STC does not require control gains $\lambda_i > 0, i = 1, 2$ to be considerably large to compensate for the disturbance's influence. However, for the convergence of HOSMO, the observer gains $K_i (i = 1, 2, 3)$ must be large instead, which still implies a risk of chattering phenomena in the control signal. This remark will be vividly illustrated in the simulation results.

4.2.3 UKF-STC Design

The application of HOSMO has partially lifted the burden of state feedback requirement for the STC design. However, HOSMO-STC still requires measurements of the vertical displacement and pitch angle of the vehicle body. This section introduces a more practical control approach, as UKF is employed to estimate the states of the system. The method uses only relative displacements that can be easily obtained from measuring suspension strokes.

1. UKF Formulation:

   UKF-oriented system state: $X = \begin{bmatrix} z_c & \dot{z}_c & \varphi & \dot{\varphi} & z_1 & \dot{z}_1 & z_2 & \dot{z}_2 \end{bmatrix}^{\mathrm{T}}$

   State transition function (discretized by the Euler method):

$$X_k = X_{k-1} + \begin{bmatrix} X_{k-1}(2) \\ (1/M)(-\phi_1 + F_1 + F_2) \\ X_{k-1}(4) \\ (1/I)(-\phi_2 + aF_1 - bF_2) \\ X_{k-1}(6) \\ (1/m_f)(k_{s1}\Delta y_1 + b_{e1}\Delta \dot{y}_1 - F_1) \\ X_{k-1}(8) \\ (1/m_r)(k_{s2}\Delta y_2 + b_{e2}\Delta \dot{y}_2 - F_2) \end{bmatrix} T_s + W \tag{21}$$

   where T_s is the sampling time, W is assumed to be an additive process noise, $W(0, Q)$. Measurement function:

$$Y = \begin{bmatrix} \Delta y_1 \\ \Delta y_2 \end{bmatrix} + V = \begin{bmatrix} z_c + a\sin\varphi - z_1 \\ z_c - b\sin\varphi - z_2 \end{bmatrix} + V \tag{22}$$

$$= \begin{bmatrix} X_k(1) + a\sin X_k(3) - X_k(5) \\ X_k(1) - b\sin X_k(3) - X_k(7) \end{bmatrix} + V = J(X_k) + V \tag{23}$$

   where $V(0, R)$ is the measurement noise.

   The standard UKF algorithm can be expressed as follows [14].

   - Initialization:

$$\hat{X}_0 = \mathrm{E}\left[X_0\right], \quad P_0 = \mathrm{E}[(X_0 - \hat{X}_0)(X_0 - \hat{X}_0)^{\mathrm{T}}]$$

   - Sigma point calculation:

$$X_{k-1} = \begin{bmatrix} \hat{X}_{k-1} & \hat{X}_{k-1} + \eta\sqrt{P_{k-1}} & \hat{X}_{k-1} - \eta\sqrt{P_{k-1}} \end{bmatrix}$$

- Time update:

$$\begin{aligned} X_{k|k-1} &= F(X_{k-1}, U_{k-1}) \\ \hat{X}_k^- &= \sum_{i=0}^{2N} \omega_i^{(m)} X_{i,k|k-1} \\ P_k^- &= \sum_{i=0}^{2N} \omega_i^{(c)} [X_{i,k|k-1} - \hat{X}_k^-][X_{i,k|k-1} - \hat{X}_k^-]^T + Q \\ Y_{k|k-1} &= J(X_{k|k-1}) \\ \hat{Y}_k^- &= \sum_{i=0}^{2N} \omega_i^{(m)} Y_{i,k|k-1} \end{aligned}$$

- Measurement update:

$$\begin{aligned} P_{\tilde{Y}_k \tilde{Y}_k} &= \sum_{i=0}^{2N} \omega_i^{(c)} [Y_{i,k|k-1} - \hat{Y}_k^-][Y_{i,k|k-1} - \hat{Y}_k^-]^{\mathrm{T}} + R \\ P_{X_k Y_k} &= \sum_{i=0}^{2N} \omega_i^{(c)} [X_{i,k|k-1} - \hat{X}_k^-][Y_{i,k|k-1} - \hat{Y}_k^-]^{\mathrm{T}} \\ \mathrm{K}_k &= P_{X_k Y_k} P_{\tilde{Y}_k \tilde{Y}_k}^{-1} \\ \hat{X}_k &= \hat{X}_k^- + \mathrm{K}_k (Y_k - \hat{Y}_k^-) \\ P_k &= P_k^- - \mathrm{K}_k P_{\tilde{Y}_k \tilde{Y}_k} \mathrm{K}_k^{\mathrm{T}} \end{aligned}$$

  where $N = 8$ is the state dimension, $\lambda = N(\alpha^2 - 1)$ and $\eta = \sqrt{N + \lambda}$ are scaling factors, and ω_i is a scalar weight set satisfying:

$$\begin{aligned} \omega_0^{(m)} = \lambda/(N+\lambda), \quad \omega_0^{(c)} = \lambda/(N+\lambda) + (1 - \alpha^2 + \beta) \\ \omega_i^{(m)} = \omega_i^{(c)} = 1/\{2(N+\lambda)\}, \quad i = 1, 2, ..., 2N \end{aligned}$$

2. UKF-STC formulation:

   With estimation results from the UKF, a sliding surface can be designed as follows:

$$\hat{S} = C_1 \hat{X}_1 + \hat{X}_2 \tag{24}$$

   where $\hat{X}_i \, (i = 1, 2)$ are the states of the system reconstructed from UKF.

   Taking the derivative of the sliding surface 24 yields:

$$\begin{aligned} \dot{\hat{S}} &= C_1 \dot{\hat{X}}_1 + \dot{\hat{X}}_2 \\ &= C_1 (\dot{X}_1 - \dot{\tilde{X}}_1) + (\dot{X}_2 - \dot{\tilde{X}}_2) \\ &= C_1 X_2 - C_1 \dot{\tilde{X}}_1 + (H + GU + D) - \dot{\tilde{X}}_2 \end{aligned} \tag{25}$$

   where $\tilde{X}_i = X_i - \dot{\hat{X}}_i$, $(i = 1, 2)$ denote UKF state estimation errors.

   From the above sliding surface derivative equation, a control law can be designed accordingly as follows.

$$U = G^{-1}(-C_1 \hat{X}_2 - \hat{H} - \hat{D} - \lambda_1 |S|^{\frac{1}{2}} sign\,(S) - \int_0^t \lambda_2 sign\,(S)\, d\tau) \tag{26}$$

   Substituting the control law 26 into 25 results in the following closed-loop dynamics:

$$\begin{cases} \dot{\hat{S}} = -\lambda_1 |S|^{\frac{1}{2}} sign(\hat{S}) + Z \\ \dot{Z} = -\lambda_2 sign(\hat{S}) + (C_1 \dot{\tilde{X}}_2 - C_1 \ddot{\tilde{X}}_1 + \dot{\hat{H}} - \ddot{\tilde{X}}_2 + \dot{\hat{D}}) \end{cases} \tag{27}$$

If the control parameters λ_1 and λ_2 are properly selected such that the effects of estimation errors $\tilde{X}_1$, $\tilde{X}_2$, $\tilde{H}$, $\tilde{D}$ are compensated, e.g. $\lambda_1 = 1.5\sqrt{\Delta_2}$ and $\lambda_2 = 1.1\Delta_2$ with $max|C_1\ddot{\tilde{X}}_1 + \dddot{\tilde{H}} - \ddot{\tilde{X}}_2 + \dddot{\tilde{D}}| \leq \Delta_2$, then the second order sliding mode will happen. Once $\hat{S} = \dot{\hat{S}} = 0$, it follows that:

$$\begin{aligned} C_1\hat{X}_1 + \hat{X}_2 &= 0 \\ C_1X_1 + \dot{X}_1 &= C_1\tilde{X}_1 + \tilde{X}_2 \end{aligned} \tag{28}$$

Assume that the UKF estimation errors are bounded satisfying $max|C_1\tilde{X}_1 + \tilde{X}_2| \leq \Delta_3$. Then, it can derive from the above equation that

$$\begin{aligned} X_1(t) &\leq \frac{\Delta_3}{C_1} - \frac{X_1(0)}{C_1}e^{-C_1t} \\ \lim_{t\to\infty} X_1(t) &\leq \lim_{t\to\infty}\left(\frac{\Delta_3}{C_1} - \frac{X_1(0)}{C_1}e^{-C_1t}\right) \leq \frac{\Delta_3}{C_1} \end{aligned}$$

where $X_1(0) = X_1(t = 0)$.

The above inequality indicates that the system states can be driven to an arbitrarily small region around the equilibrium, provided that the UKF are well tuned and a sufficiently large control gain C_1 is selected. Moreover, the benefit of a sufficiently large control gain C_1 is twofold. It not only shortens the state convergence time but also minimizes the steady-state stabilizing errors of the system.

5 Simulation Results and Discussion

5.1 Road profile and parameter selection

To evaluate the performance of the proposed control algorithms, the half-car suspension system and three control candidates are constructed in the MATLAB-Simulink environment. Table 1 summarizes the values of all parameters used for system modeling. The classical bumped road profiles chosen to verify

Table 1: Nominal parameters used for modeling the half-car suspension system.

Parameter	Value	Parameter	Value
M	$1200\,kg$	I	$600\,kgm^2$
m_f	$100\,kg$	m_r	$100\,kg$
k_{s1}	$15000\,N/m$	k_{s2}	$15000\,N/m$
b_{e1}	$2500\,Ns/m$	b_{e2}	$2500\,Ns/m$
k_{t1}	$2\times10^5\,N/m$	k_{t2}	$2\times10^5\,N/m$
b_{t1}	$1000\,Ns/m$	b_{t2}	$1000\,Ns/m$
a	$1.2\,m$	b	$1.5\,m$

the effectiveness of the proposed controllers are borrowed from [1] and of the following form.

$$z_{oi} = \begin{cases} \frac{h_b[1-cos(6\pi t)]}{2}, & t \in \mathrm{T}_i \\ 0, & \text{otherwise} \end{cases} \tag{29}$$

where $z_{oi}(i = 1, 2)$ represent the ground displacement inputs to the front and rear wheel, respectively. $h_b = 2\,\mathrm{cm}$ denotes the magnitude of the bump road. $T_i\,(i = 1, 2)$ denotes the time periods for the front

and rear wheels, that is, $T_1 = [1,\ 1.25]$ and $T_2 = [1 + \Delta_t,\ 1.25 + \Delta_t]$. $\Delta_t = (a+b)/V_0$ stands for the time constant between the front and rear wheel with $V_0 = 20\,m/s$ is the constant speed of the vehicle.

Table 2 records the control gains dedicated to each control candidate. In addition to that, a process noise covariance $Q = 10^{-8} \times diag([0.1, 1, 0.1, 1, 1, 5 \times 10^{10}, 5 \times 10^{10}])$ and a measurement noise covariance of $R = 10^{-6} \times diag([1, 1])$ are selected by the trial and error method for the UKF.
The principal sampling time is chosen to be $10^{-4}\,(s)$, and the ODE4 Runge-Kutta is set to be the solver.

Table 2: Selection of control parameters for three candidates for the control algorithm.

Parameters	FS-STC	HOSMO-STC	UKF-STC
C_1	15	15	15
λ_1	$1.5 \times \sqrt{300}$	2	$1.5 \times \sqrt{20}$
λ_2	1.1×300	2	1.1×20
K_1		$4 \times 65^{1/3}$	
K_2		$11 \times 65^{1/2}$	
K_3		4×65	

5.2 Comparative Simulation Results

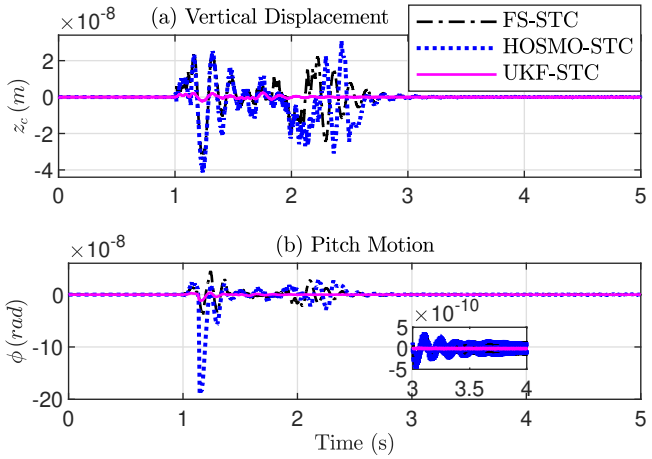

Figure 2: Stabilization performance of three considered controllers. (a) Vertical displacement. (b) Pitch motion

Figure 2 demonstrates vertical displacement and pitch angle stabilization precision of the three controllers. It is easy to point out that UKF-STC outperforms FS-STC and HOSMO-STC in terms of both convergence time and accuracy. UKF-STC trajectory also exhibits much less chattering than the other two counter parts.

Figure 3 illustrates the vertical and pitch acceleration time record, which is believed to directly affect driving comfort. It can be seen from Figure 3 that UKF-STC exhibits superior performance in acceleration minimization compared to the other two control algorithms. Figure 3 also shows the undesired chattering phenomena in the trajectories of FS-STC and HOSMO-STC even after contact time with the bumped part of the road. Meanwhile, UKF-STC does not suffer from this phenomenon and shows almost consistency in its trajectories.

Safety concerns can be assessed in Figure 4, where the ratios of dynamic and static loads of all controller candidates are compared. It can be interpreted from Figure 4 that all controllers satisfy the

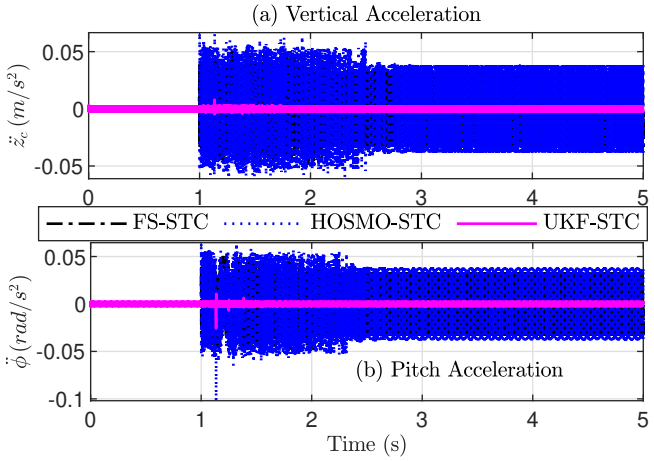

Figure 3: Riding comfort in terms of acceleration minimization. (a) Vertical acceleration. (b) Pitch acceleration.

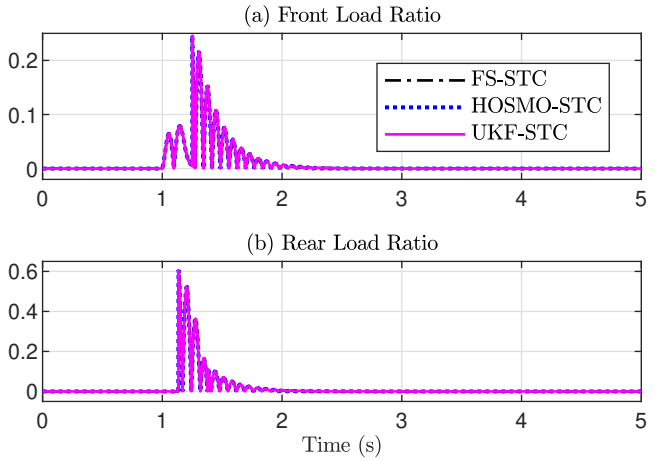

Figure 4: Road holding with dynamic and static loads ratio. (a) Front wheel. (b) Rear wheel.

safety constraint since the load ratios are all less than 1.

The control signal trajectories, which represent the ideal force generation of all control algorithms, are depicted in Figure 5. Although their overall shapes are similar, there is a striking difference in their magnitude. Specifically, both FS-STC and HOSMO-STC exhibit considerably larger chattering effect in their control signals compared to UKF-STC. The chattering in their trajectories might pose a serious challenge when the actuator dynamics is considered and designed to track these ideal forces.

The state estimation accuracy of HOSMO and UKF are shown in Figure 6 and Figure 7, respectively. The chattering phenomenon in the trajectory can be seen for the case of HOSMO but not for the case of UKF indicates that UKF has better state estimation performance.

The comparison of Figure 2 and Figure 8 shows the interesting fact that, even though the relative displacements of the three controllers are remarkably similar, their vertical displacements and pitch angles can be significantly different from each other. This observation suggests that directly using the relative displacement feedback and stabilizing it cannot guarantee the stabilization of vertical displacement and pitch angle. This method also lacks mathematical justification as

$$\Delta_{y1} = z_c + asin\varphi - z_1 = 0$$
$$\Delta_{y2} = z_c - bsin\varphi - z_2 = 0$$

is a set of two equations with four variables, thus implying no unique solutions. z_c, φ and z_i, $i = 1, 2$ could continue to vary without convergence to zero in such a way that they still satisfy the equation set. For example, a set of solutions could be $\varphi = 0$ and $z_c = z_1 = z_2 = \xi_z$, where ξ_z is an arbitrary constant.

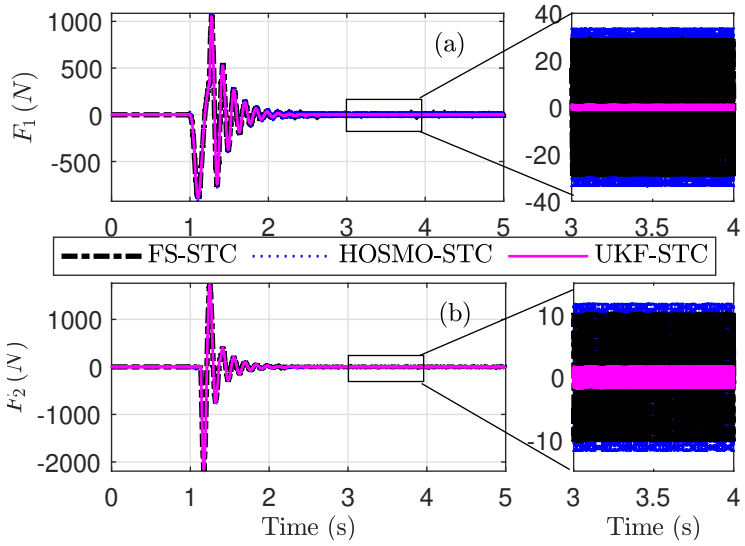

Figure 5: Control inputs in the form of ideal force generation. (a) Front wheel. (b) Rear wheel.

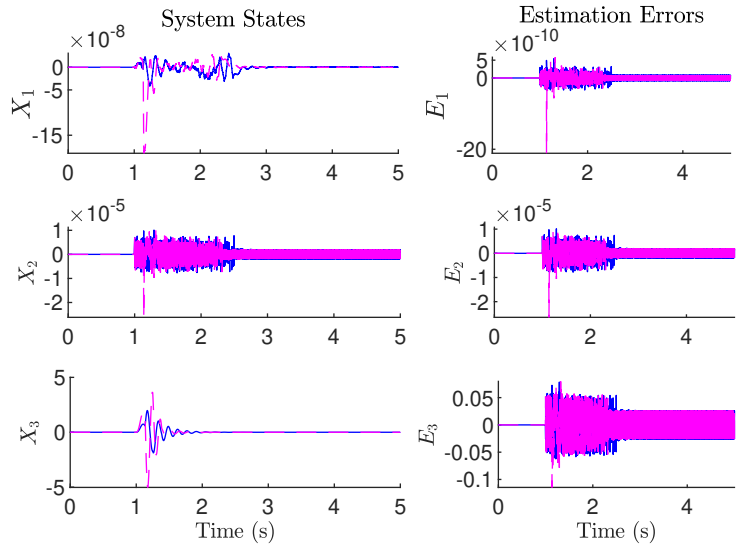

Figure 6: State estimation performance of HOSMO with state trajectories on the left and estimation errors on the right side of the figure.

Finally, Figure 9 captures the stabilization effectiveness of three controllers in noisy measurement, where a measurement noise of $2 \times 10^{-5}\, m$ is added to the system output. It is evident that compared to Figure 2, their performance degrades significantly in the presence of noise. However, UKF-STC performance is still comparable to that of HOSMO-STC and FS-STC. In addition, the UKF-STC trajectory is more stable compared to others.

5.3 Discussion

The comparative simulation results have demonstrated the superiority of UKF-STC over FS-STC and HOSMO-STC in suspension stabilization. This result can be explained as follows. Although FS-STC has both displacement and velocity measurements, the ignorance of lumped disturbance in control design 10 force its control gains λ_i, $i = 1, 2$ to be significantly large enough to compensate for the influence of disturbance. Similarly, in HOSMO-STC, the observer gains K_i, $i = 1, 2, 3$ from HOSMO 12 must be sufficiently large for disturbance compensation. Those large control/observer gains magnify the undesired

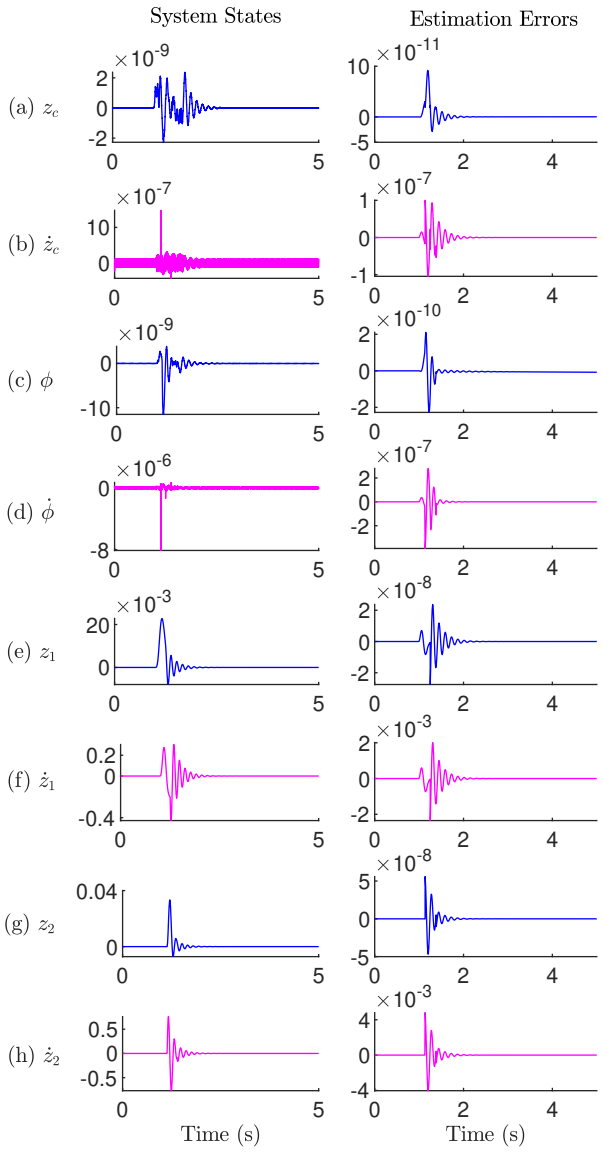

Figure 7: State estimation performance of UKF with states on the left side and their estimation errors on the right side.

chattering effects of the *sign* function, thus degrading the control performance. On the other hand, UKF-STC utilizes UKF to reconstruct system state and disturbances and uses estimation results for control design. Consequently, UKF-STC has higher accuracy, and its control gains are allowed to be relatively small, resulting in less chattering.

The advantages and limitations of each control candidate are summarized below.

1. FS-STC:
    - Advantage: control design process is straight-forward without the need for state estimation
    - Disadvantage: FS-STC requires both displacement and velocity measurements for vertical and pitch motions. Control gains associating with the *sign* function must be sufficiently large to compensate for the lumped disturbance, thus increasing chance of chattering phenomenon.

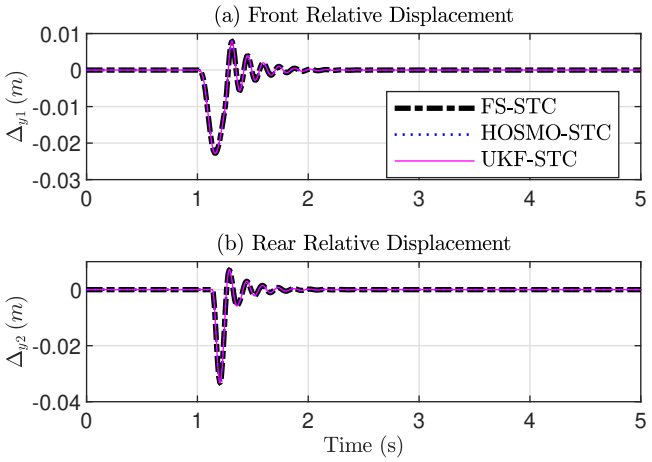

Figure 8: Front and rear relative suspension displacements of three control candidates.

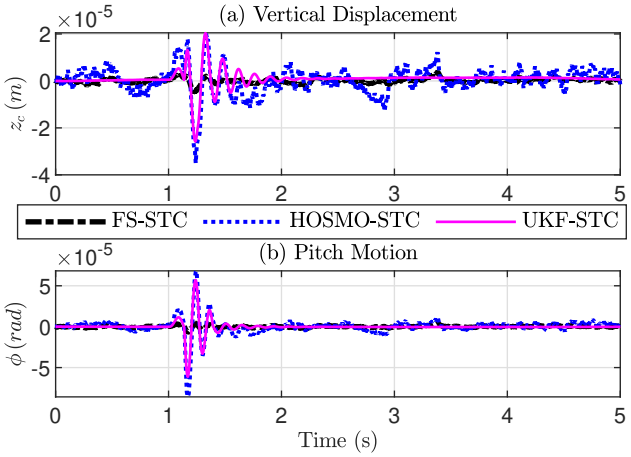

Figure 9: Stabilization performance affected by noisy measurement. Magnitude of noise: 2×10^{-5}.

2. HOSMO-STC:

   - Advantage: vertical and pitch velocity values are estimated, thus being less dependent on state feedback information. Control gains are consequently smaller compared with FS-STC.
   - Disadvantage: vertical and pitch displacement sensors are required. Sufficiently large observer gains must be selected to compensate for disturbances, which still leads to chattering phenomenon in control signals.

3. UKF-STC:

   - Advantage: UKF-STC does not require direct displacement and velocity measurements of vertical and pitch motions but uses the more-practical and common relative displacement (suspension stroke) sensings. All system states can be estimated by UKF and then utilized for dynamics and disturbance compensation, thus increasing accuracy, decreasing control gains, lowering chattering chance of happening.
   - Disadvantage: Since the control design is indirect via state estimate, its performance strongly depends on UKF's state estimation. Thus, careful parameter tuning is required for high precision.

6 Conclusion, future work and learned lesson

This study tackles the task of stabilizing a non-linear half-car suspension system while considering the availability of state feedback information. STC, which requires both displacement and velocity feedback, has been selected as the main control algorithm to achieve the stabilization, driving comfort and road holding objectives. As a result, HOSMO and UKF are subsequently employed to reduce the dependence on state feedback measurement. While HOSMO-STC requires only direct measurement of vertical displacement and pitch angle, UKF-STC utilizes more readily accessible relative displacement such as suspension strokes. The results of the comparative simulation have shown that the proposed UKF-STC outperforms the other two controllers in terms of convergence time, accuracy, and chattering attenuation. Some limitations that can be addressed in future work are listed below.

- The effect of noise and the influence of parameter uncertainty onto the accuracy of observer/filter and consequently the performance of the control system requires more intensive assessment.
- A guideline on how to tune the process/measurement noise covariance of the UKF is missing.
- Actuator dynamics should be considered in system modeling and controller design.

Several lessons have been taken from this study. Specifically, the study requires us first to understand the dynamics of the half-car suspension system. Second, the obtained dynamic equations need to be transformed into a control-oriented modeling readily suitable for control application. Third, we are urged to assess the availability of system states and figure out solutions such as the implementation of filters or observers for missing information. Finally, limitations of the outcomes helps us plan for future research work.

References

[1] W. Sun, H. Pan, and H. Gao, "Filter-based adaptive vibration control for active vehicle suspensions with electrohydraulic actuators," *IEEE Transactions on Vehicular Technology*, vol. 65, no. 6, pp. 4619–4626, 2015.

[2] H. Pan, W. Sun, X. Jing, H. Gao, and J. Yao, "Adaptive tracking control for active suspension systems with non-ideal actuators," *Journal of Sound and Vibration*, vol. 399, pp. 2–20, 2017.

[3] H. Yan, J. Sun, H. Zhang, X. Zhan, and F. Yang, "Event-triggered h_∞ state estimation of 2-dof quarter-car suspension systems with nonhomogeneous markov switching," *IEEE Transactions on Systems, Man, and Cybernetics: Systems*, vol. 50, no. 9, pp. 3320–3329, 2018.

[4] H. Pang, X. Zhang, and Z. Xu, "Adaptive backstepping-based tracking control design for nonlinear active suspension system with parameter uncertainties and safety constraints," *ISA transactions*, vol. 88, pp. 23–36, 2019.

[5] H. Pan, X. Jing, W. Sun, and H. Gao, "A bioinspired dynamics-based adaptive tracking control for nonlinear suspension systems," *IEEE transactions on control systems technology*, vol. 26, no. 3, pp. 903–914, 2017.

[6] J. J. Rath, M. Defoort, H. R. Karimi, and K. C. Veluvolu, "Output feedback active suspension control with higher order terminal sliding mode," *IEEE Transactions on Industrial Electronics*, vol. 64, no. 2, pp. 1392–1403, 2016.

[7] M. Papadimitrakis and A. Alexandridis, "Active vehicle suspension control using road preview model predictive control and radial basis function networks," *Applied Soft Computing*, vol. 120, p. 108646, 2022.

[8] J. Wang, F. Jin, L. Zhou, and P. Li, "Implementation of model-free motion control for active suspension systems," *Mechanical Systems and Signal Processing*, vol. 119, pp. 589–602, 2019.

[9] J. Davila, L. Fridman, and A. Levant, "Second-order sliding-mode observer for mechanical systems," *IEEE transactions on automatic control*, vol. 50, no. 11, pp. 1785–1789, 2005.

[10] A. Levant, "Robust exact differentiation via sliding mode technique," *automatica*, vol. 34, no. 3, pp. 379–384, 1998.

[11] J. A. Moreno and M. Osorio, "Strict lyapunov functions for the super-twisting algorithm," *IEEE transactions on automatic control*, vol. 57, no. 4, pp. 1035–1040, 2012.

[12] A. Chalanga, S. Kamal, L. M. Fridman, B. Bandyopadhyay, and J. A. Moreno, "Implementation of super-twisting control: Super-twisting and higher order sliding-mode observer-based approaches," *IEEE Transactions on Industrial Electronics*, vol. 63, no. 6, pp. 3677–3685, 2016.

[13] A. Levant, "Higher-order sliding modes, differentiation and output-feedback control," *International journal of Control*, vol. 76, no. 9-10, pp. 924–941, 2003.

[14] R. Van Der Merwe and E. A. Wan, "The square-root unscented kalman filter for state and parameter-estimation," in *2001 IEEE international conference on acoustics, speech, and signal processing. Proceedings (Cat. No. 01CH37221)*, vol. 6. IEEE, 2001, pp. 3461–3464.